NOTICE CONCERNING COPYRIGHT RESTRICTIONS

Characterization of Induced Seismicity near an Injection Well at the Northwest Geysers Geothermal Field, California

Gisela Viegas and Lawrence Hutchings

Lawrence Berkeley National Laboratory, Berkeley CA

Keywords

Geysers, micro-earthquakes, induced seismicity, earthquake source, stress drop, radiated energy, Empirical Green's function

ABSTRACT

We investigate the temporal and spatial dependence of source parameters of micro-earthquakes (<M3) before and during water injection at the Northwest Geysers between 2005 and 2010. Our objective is to understand the relation among injection, production and source mechanisms of micro-earthquakes. We examine a small area that surrounds an injection well (Prati 9) that extends into the deep zone. We utilize three approaches to determine the source parameters of the micro-earthquakes; the Empirical Green's Function (EGF) method (Viegas *et al.*, 2010), NetMoment method (Hutchings 2002), and moment tensor inversion (Minson and Dreger, 2008). We first compare the source parameters of 30 earthquakes determined using the three approaches for validation purposes, and then we determine the source parameters for all the earthquakes located within a small volume around the well head before and during injection. We find a good correlation coefficient of 91% between the monthly water injection-rate and the number of induced micro-earthquakes located inside the small volume, with a zero time lag, indicating that the seismic response to water injection is less than a month time. We find the *b*-value in the Gutenberg−Richter law, which equates the proportion of small earthquakes to large ones, increased from 1.3 to 1.6 with the start of water injection, indicating an increase of the number of small earthquakes relative to larger earthquakes due to reservoir stimulation. Our results indicate that micro-earthquakes at the Northwest Geysers have on average stress drops (mean of 11 MPa) comparable to the ones of natural occurring tectonic earthquakes in the region (around 17 MPa). We notice that the shape of the earthquake cloud is slightly elongated in the SW-NE direction, consistent with the preferential alignment direction of micro-cracks found in anisotropic studies, indicating that slip is being facilitated in pre-existing cracks. The study of micro-seismicity is a useful tool in reservoir exploration management, as it can be used to track the release of strain and the injected fluid flow paths, and to characterize the permeability of the reservoir. The source information has implications for understanding the physics of faulting and the principal mechanisms involved in induced seismicity.

Introduction

We investigate the source mechanisms of micro-earthquakes at the Northwest Geysers geothermal field in California between 2005 and 2010. Our objective is to understand the relation among injection, production and source mechanisms of micro-earthquakes. The injection of water into the ground has become a common procedure in the management of geothermal reservoirs. At The Geysers, which is a vapor dominated reservoir, the injection of water has improved productivity of the reservoir and extended the lifespan of an economically viable energy production activity. Water injection helps maintain the reservoir pressures and the flow rates at production wells, and improves the chemical quality of the steam. (Majer and Peterson, 2007a). However, the injection of water also produces an increase in micro-seismicity. The relationship between water injection and increased micro-seismicity at The Geysers has been established in many studies (*e.g.* Eberrhart-Phillips and Openheimer, 1986; Smith *et al.*, 2000), showing a good correlation between the injection flux and the rate of increased micro-seismicity. Micro-seismicity is used as a tool in exploration management, as it can be used to track the release of strain and the injected fluid flow paths, and to characterize the permeability of the reservoir. However, the level of increased micro-seismicity has generated concerns among the nearby communities. The mechanism by which the micro-seismicity is triggered is not clear, and several possible mechanisms are considered. The presence of fluids perturbs the stress field (by changing the pore pressure) and/or facilitates chemical reactions that alter the frictional properties of the reservoir (by, for example, the precipitation of cements that bonds fracture walls; *e.g.*, Karner, 2005). The injection of cold water into the reservoir may activate the thermal contraction of the rock either on pre-existing fractures, facilitating the slip, or generating new fractures (Majer and Paterson, 2007a). Poroelastic

stressing is proposed as a production induced mechanism due to the reservoir contraction by the extraction of steam. Source information of both induced and tectonic micro-earthquakes at The Geysers will help constrain the possible mechanisms of the induced micro-seismicity, allowing for a more efficient reservoir management and a more realistic seismic potential assessment.

In this study, we investigate how micro-seismicity evolves within a small crustal volume which surrounds a water injection well from 2005 to 2010. We estimate the source parameters of micro-earthquakes which occurred before and during the injection of water and look for the temporal variations of the micro-earthquake source parameters.

Retrieving source parameters of micro-earthquakes such as fault radius, stress drop, seismic moment and radiated energy is challenging because it requires the analysis of high frequency energy which is heavily attenuated as the waves propagate throughout the medium. To estimate the source parameters of the micro-earthquakes at The Geysers we use three techniques: the Empirical Green's Function (EGF) method, the NetMoment method; and the Moment Tensor (MT) inversion method (Minson and Dreger, 2008). We use the EGF method, which empirically corrects for attenuation and site effects, as a validation tool for the NetMoment method, which simultaneously inverts for micro-earthquake source properties and medium attenuation (Gok *et al.*, 2009). The EGF method is of limited application because it requires the use of a smaller micro-earthquake with certain characteristics as a medium transfer function, and that EGF earthquake is not always available. The NetMoment method is automated and particularly useful when dealing with large datasets (Hutchings *et al*., 2010) but carries larger uncertainties in the site and attenuation corrections than the EGF method. We use the MT inversion method to obtain full second-order moment tensor solutions. The moment tensor gives information on the fracture plane and faulting mechanism. Substantial volumetric components have been found for earthquakes in geothermal and volcanic environments (*e.g.*, Julian *et al.*, 1998), including The Geysers (Boyd 2011, Ross *et al.*, 1996) indicating a tensile component in the mechanism of fracture, or with non-planar fault geometries. The volumetric component of earthquakes in these environments is possibly associated with the presence of fluids which perturb the stress field and facilitate chemical reactions that alter the frictional properties of the reservoir, or with thermal contraction due to reservoir cooling. Most moment tensor inversion methods limit the source to a pure shear mechanism, and first motion methods poorly resolve the volumetric component, even when the station coverage is good. We investigate the source mechanism of the micro-earthquakes at The Geysers applying a 3-component full-waveform inversion to obtain moment tensors.

Our goal is to characterize the source characteristics of the tectonic and induced micro-earthquakes at The Geysers and to understand how local stresses change as a result of water injection and steam extraction, the most common activities in geothermal energy production.

Data

We use micro-earthquake data from The Geysers recorded and processed by the Lawrence Berkeley National Laboratory (LBNL). LBNL runs a seismic array at The Geysers which consists of thirty 3-component short-period stations that continually telemeter digital data sampled at 500 samples per second to a central acquisition computer (Majer *et al.*, 2007a). The seismic array has been continually recording data since the end of 2003. The number of stations increased over the years from an initial number of 23 to the current number of 30. The micro-earthquake recordings are processed using LBNL's automated data processing system, designated by Rapid Reservoir Assessment System (RRAS; Jarpe *et al.*, 2011, Hutchings *et al.*, 2011). The automated system simultaneously relocates the micro-earthquakes and performs a tomographic inversion. It outputs a catalog with micro-earthquake locations, moments and magnitudes, and a 3D-velocity structure (V_p and V_s) of The Geysers. In this study we use the micro-earthquake catalog data and the crustal velocity model resulting from the RRAS processing.

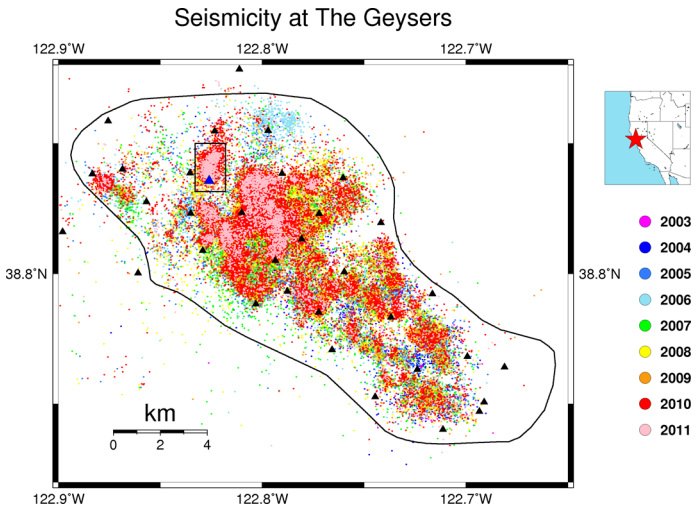

Figure 1. Seismicity map of The Geysers from 2003 to 2011. The earthquakes (dots) are color coded by year, with more recent earthquakes being plotted on top of previous ones. Also shown are the boundary outline of The Geysers geothermal field, the location of the seismic stations (black triangles), the location of the well-head of the injection well Prati 9 (blue triangle), and the rectangular box surrounding well Prati 9 that defines our study area. The red star on the inset map indicates The Geysers location within the state of California.

In 2003, wastewater from Santa Rosa, CA, started to be directly injected through a pipeline, with an initial average flux of 41 million liters per day (Majer *et al.*, 2007a). The micro-seismic activity is significant at The Geysers as a result of the geothermal exploration. More than 19,000 micro-earthquakes were reported in 2006, 99% of which with magnitudes smaller than M2 (Majer *et al.*, 2007b). Figure 1 maps the micro-seismic activity at The Geysers from 2003 to 2011 and the current LBNL seismic station configuration. The good correlation between water injection and steam production with increased seismicity is well documented at The Geysers (*e.g.* Eberrhart-Phillips and Openheimer, 1986; Smith *et al.*, 2000). We focus our micro-earthquake study to a small volume which contains the injection well Prati 9 and the micro-earthquake cloud induced by water injection (Figure 1). Prati 9 is located in the NW region of The Geysers. It was drilled in 1983, explored as an injection well for a few years from 1989 to 1990 and from 1991 to 1996, and plugged and abandoned in 2001. It

was re-opened in 2007, cleaned and drilled deeper (from 8972.7 to 9647.2 feet deep relative to the top of the Kelly bushing, which is 30 feet above the ground). Injection of water started in November 2007 and is ongoing (as of May 2011). There was no injection in nearby wells, so that the micro-seismicity cloud is solely induced from water injection in Prati 9. In April 2010 Calpine started injecting water in Prati 29, a well located a few hundred meters NE of Prati 9. After that, the cloud of micro-earthquakes induced by water injection in both wells becomes indistinguishable. Because of this, we only study micro-earthquakes which occurred up to April 15 2010, so that we can understand the spatial and temporal evolution of micro-seismicity due to the injection of water at one single source.

Correlation of Micro-Seismicity with Water Injection Rate

Figure 2 shows the spatial and temporal variation of micro-seismicity inside our study volume which contains the injection well Prati 9 and extends into the deep zone. An increase in micro-seismicity bellow the bottom hole of the injection well is observed as soon as injection starts in November 2007. A small cloud of micro-earthquakes develops bellow the bottom of the well and is maintained throughout the injection period. It has a oval shape, vertical elongated with about 1.5 km of vertical length by 1 km x 1 km of lateral length. Most micro-seismicity prior to injection is shallower than the bottom of the well. Most of the micro-earthquakes that occurred in 2006 are aftershocks of a M3 which occurred adjacent to our study volume on May 12. The aftershock activity occurred mostly within 2 days of the mainshock.

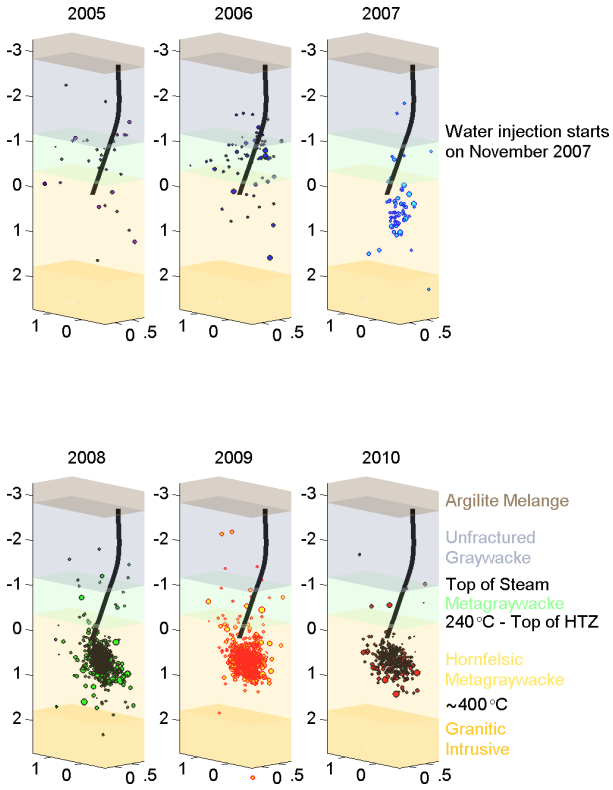

Figure 2. 3D view of the spatial distribution of the micro-seismicity at the Northwest Geysers in a volume surrounding the injection well Prati 9, by year, from January 2005 to April 2010. The black line shows the well depth profile. X, Y and Z are in km, and zero (the center of the coordinate system) is positioned at the bottom of the well. The sizes of the micro-earthquake circles are determined by their magnitude, which vary from M0 to M3. The different geological structures within the volume are identified by different colors. The profile was made based on a geological map supplied by Calpine. The depth of the Granitic Intrusive (Felsite) is not known in this volume and was plotted bellow the micro-earthquake cloud. Also shown are the temperatures and locations of the Top of the Steam and Top of the High Temperature Zone (HTZ) boundaries. Ground elevation is 2176 feet above sea level.

We find good correlation coefficients of 91% and 87% between the number of induced micro-earthquakes located inside the study volume and the monthly water injection-rate, and between the number of micro-earthquakes and the gross volume of injected water, respectively (Figure 3). Both cross-correlation coefficients have a zero time lag, indicating that the seismic response to water injection is less than a month time.

To quantify the change in micro-seismicity due to the injection of water, we calculate the Gutenberg-Richter relationship for the micro-earthquakes which occurred within the whole study volume before injection started and within the volume bellow the High Temperature Zone during the injection period (Figure 4). We find the *a*-value in the Gutenberg–Richter relationship, which corresponds to the expected cumulative number of earthquakes of magnitude larger or equal to zero for a complete catalog increases from 2.9 to 5.1, reflecting the onset of induced micro-seismicity. We find the *b*-value in the Gutenberg–Richter relationship, which equates the proportion of small earthquakes to large ones, increased from 1.3 to 1.6 with the start of water injection, indicating an increase of the number of small earthquakes relative to larger earthquakes due to reservoir stimulation.

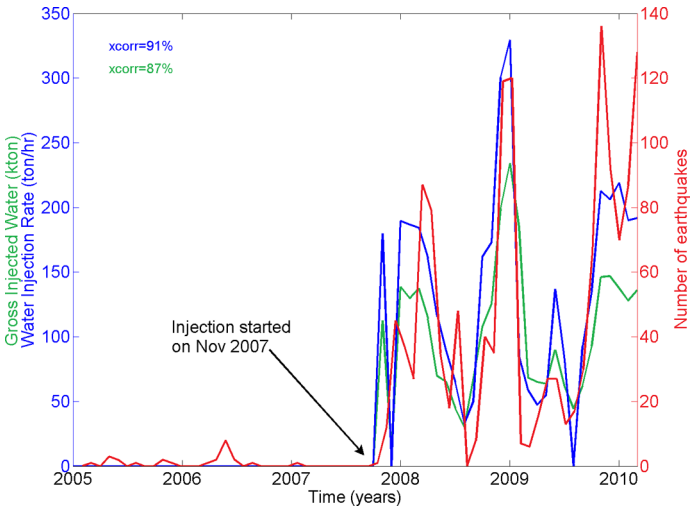

Figure 3. Total number of earthquakes per month inside our study volume (red line, right axis) and monthly gross volume of injected water in well Prati 9 (green line, left axis) and injection rate during the same time period (blue line, left axis). The two numbers on the top left correspond to the cross-correlation coefficient between the number of earthquakes and the injection rate (blue) and the number of earthquakes and the amount of injected water (green).

So, there is an increase in micro-seismicity, particularly of earthquakes with magnitudes smaller than two. We investigate the spatial distribution of the micro-seismicity and its relationship with

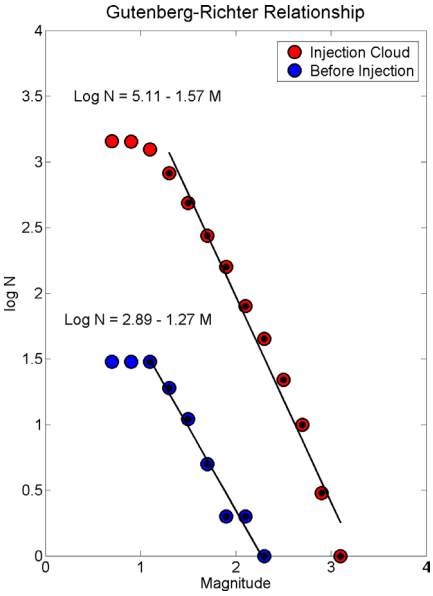

Figure 4. Gutenberg-Richter relationship for the micro-earthquakes which occurred within the whole study volume before injection started (blue) and within the volume bellow the High Temperature Zone during the injection period (red). Black dots inside the colored circles indicate the line points used in the best fit regression.

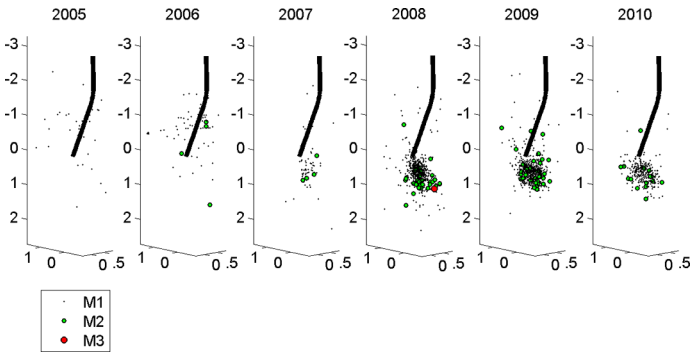

Figure 5. 3D view of the spatial distribution of the micro-seismicity within our study volume at the Northwest Geysers, by year, from January 2005 to April 2010, color coded by micro-earthquake magnitude.

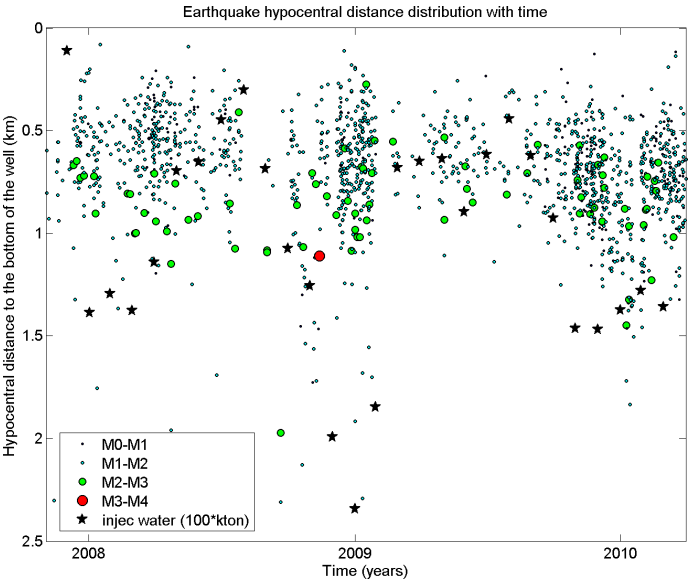

Figure 6. Time variation of the hypocentral distance of the micro-earthquakes within the induced cloud relative to the bottom of the well. The micro-earthquakes (circles) are color coded by magnitude. The starts correspond to the monthly gross volume of water injected in the well.

the injection rate. We also investigate the relative location of the >M2 micro-earthquakes within the induced micro-earthquake cloud. Figure 5 shows the micro-seismicity distribution by magnitude and Figure 6 shows the relative distance of the micro-earthquakes to the bottom of the injection well. We can see that M2 earthquakes and larger are on average located more distant from the bottom of the well than smaller magnitude micro-earthquakes. The larger micro-earthquakes occur close to the outskirts of the micro-earthquake cloud. We recall that the micro-earthquake cloud does not have a spherical shape, being more oblong in the vertical direction, so the horizontal distances, although corresponding to the cloud limits, will have smaller distances when comparing with deeper micro-earthquakes within the cloud. The average radius of the micro-earthquake cloud also seems to increase with increasing volume of injected water, and decrease when less water is injected. The number of >=M2 micro-earthquakes also correlates well with the volume of injected water. In summary, the micro-earthquake cloud expands and collapses depending on the volume of water being injected, with the larger micro-earthquakes occurring mostly at the cloud boundary. We notice that the shape of the earthquake cloud is slightly elongated in the SW-NE direction, consistent with the preferential alignment direction of micro-cracks found in anisotropic studies (Evans *et al.*, 1995; Elkibbi *et al.*, 2005), indicating that slip may be being facilitated in pre-existing cracks. The following micro-earthquake source parameter study may help shed some light on the primary faulting mechanism and on whether new cracks are being formed or slip is being accommodated in pre-existing cracks.

Source Methods – EGF and NetMoment

To investigate the source characteristics of the micro-earthquakes at The Geysers (*e.g.*, fault radius, stress drop, seismic moment and radiated energy) we use two methods: the Empirical Green's Function (Mori and Frankel, 1990; Hutchings and Wu, 1990); and the NetMoment method (Hutchings, 2002). As mentioned in the introduction, we use the EGF method to validate the results of the NetMoment method by comparing the source parameters results of micro-earthquakes used in both studies. We follow the methodology adopted in previous studies for both methods (*e.g.*, EGF - Viegas *et al.*, 2010, and Viegas, 2011; and NetMoment - Hutchings, 2002), and its application to The Geysers dataset has been already detailed described by Viegas and Hutchings, (2010). Here we give just a brief overview of the two methods. Both methods are applied in the frequency domain. The EGF method uses a small earthquake as a transfer medium, and the source parameters are obtained by fitting the spectral ratio of the displacement spectra of both earthquakes. First we solve for the corner frequency of both large (f_{c1}) and small (f_{c2}) micro-earthquakes and for the relative long period level of the ratio between the two micro-earthquakes (Ω_{0r}) by fitting the amplitude spectral ratio (Ω_r) using (Abercrombie and Rice, 2005),

$$\Omega_r(f) = \Omega_{0r}\left[\frac{1+\left(\frac{f}{fc_2}\right)^{\gamma n}}{1+\left(\frac{f}{fc_1}\right)^{\gamma n}}\right]^{\frac{1}{\gamma}}, \qquad (1)$$

where f is the frequency, and γ and n are constants (γ = n = 2) that controls the shape of the spectrum curvature around the corner frequency and the high frequency fall off, respectively. In many cases the corner frequency of the EGF micro-earthquake is outside of the usable bandwidth, and is indeterminate. In a second step, we fix the corner frequency of the micro-earthquake of interest, and fit the instrument-corrected displacement spectrum (Ω) solving for the long period level (Ω_0) and the combined site-specific and whole-path attenuation at station i, (κ_i) using (Boatwright, 1980),

$$\Omega(f) = \frac{\Omega_0 \exp(-\pi f \kappa_i)}{\left[1 + \left(\frac{f}{f_c}\right)^{\gamma n}\right]^{\frac{1}{\gamma}}} \quad (2)$$

In the NetMoment method, we simultaneously fit the instrument-corrected displacement spectra at all the stations, solving for the corner frequency of the micro-earthquake (f_c), the long period level (Ω_0) and the combined site-specific and whole-path attenuation at each station i, (κ_i).

In Figure 7 we show the location within our study volume of the micro-earthquakes for which source parameters are determined with both methods. In figure 8 we show the corner frequency measurements for the micro-earthquakes common to both studies and all the micro-earthquakes analyzed with the automated NetMoment method. We see that the scatter is larger for the corner frequencies determined with the EGF method, and also that this method limits the magnitude range of the micro-earthquakes that can be analyzed. The NetMoment results seem compatible with the EGF results, although on the lower bond, and we observed constant scaling with micro-earthquake size.

Attenuation Quality Factor

The attenuation quality factor (Q) is calculated from κ_i, $Q = t_i / \kappa_i$ where t_i is the travel time of the wave of interest (P or S) from the source to the station. Figure 9 shows Q obtained with both EGF and NetMoment methods. We can see that similar attenuation values are obtained with both methods, indicating that the NetMoment method is accurately correcting for attenuation. We observe that Q is not constant with varying hypocentral distance, as it is usually observed. This happens because the closest stations are almost directly on top of the hypocentral locations of the micro-earthquakes, and the path traveled by the propagating waves is mostly trough the surface layers, where most of the attenuation occurs. At more distant stations, the waves spend more time propagating in the deeper layers, where attenuation is weaker. We also observe that the attenuation of the P waves is higher than that of the S waves for the same hypocentral distances (Qp is lower than Qs), which is not usually the case and may be related with the presence of fluids.

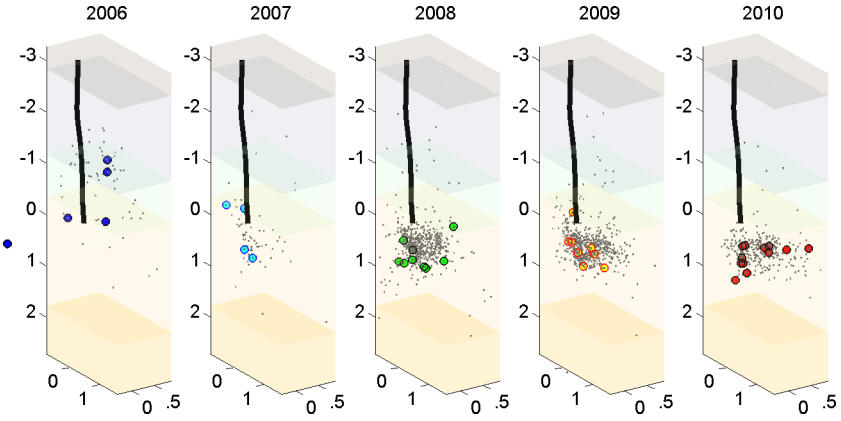

Figure 7. 3D view of the location of the micro-earthquakes for which source parameters are determined using both methods – EGF and NetMoment.

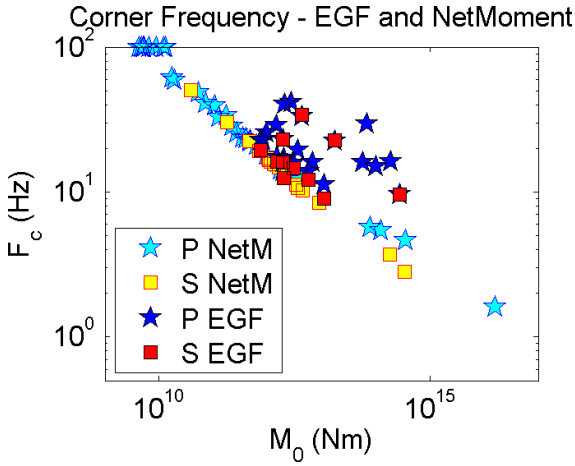

Figure 8. Corner frequency measurements for micro-earthquakes at The Geysers using two methods – EGF and NetMoment.

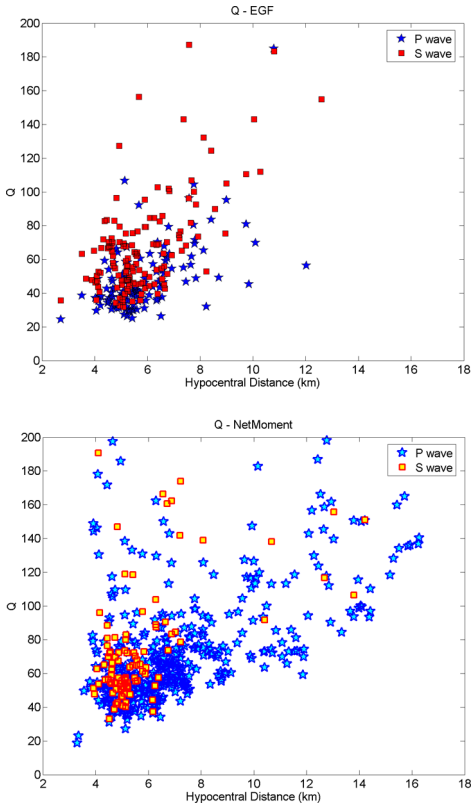

Figure 9. Attenuation quality factor obtained for P and S waves using the EGF method (top) and the NetMoment method (bottom).

Static Stress Drop

We calculate the static stress drop ($\Delta\sigma$) or stress released by faulting from our corner frequency measurements and from the seismic moment (M_0) values obtained from the RRAS catalog, using Eshelby's (1957) circular static crack solution

$$\Delta\sigma = \frac{7}{16}\frac{M_0 f_c^3}{k^3\beta^3}, \quad (3)$$

assuming Madariaga's (1976) dynamic solution for a circular fault model. k is a constant (k = 0.32 for P waves and k = 0.21 for S waves) and β is the S wave velocity.

Our results indicate that micro-earthquakes at the Northwest Geysers have on average stress drops (mean of 11 MPa) comparable to the ones of natural occurring tectonic earthquakes in the region (around 17 MPa).

Radiate Energy

After we validate the NetMoment corner frequency and attenuation corrections, we calculate the micro-earthquake radiated energy (E_S) for all the micro-earthquakes in the dataset, using the NetMoment method. To calculate the radiated energy, we integrate de velocity spectra squared, after correcting for attenuation, geometrical spreading, near-surface effect and radiation pattern. Figure 10 shows our results plotted together with a compilation of studies. We obtain high radiated energy values for the micro-earthquakes at The Geysers, but still comparable to the values obtained for natural occurring earthquakes. The high radiated energy values, associated with "normal" stress drop values, indicates that a large part of the energy budget is spent in radiated energy and not in generating new surfaces or in friction (heating), favoring the hypotheses of slip on pre-existing cracks. The moment tensor solution for these micro-earthquakes will provide more information in identifying the faulting mechanism.

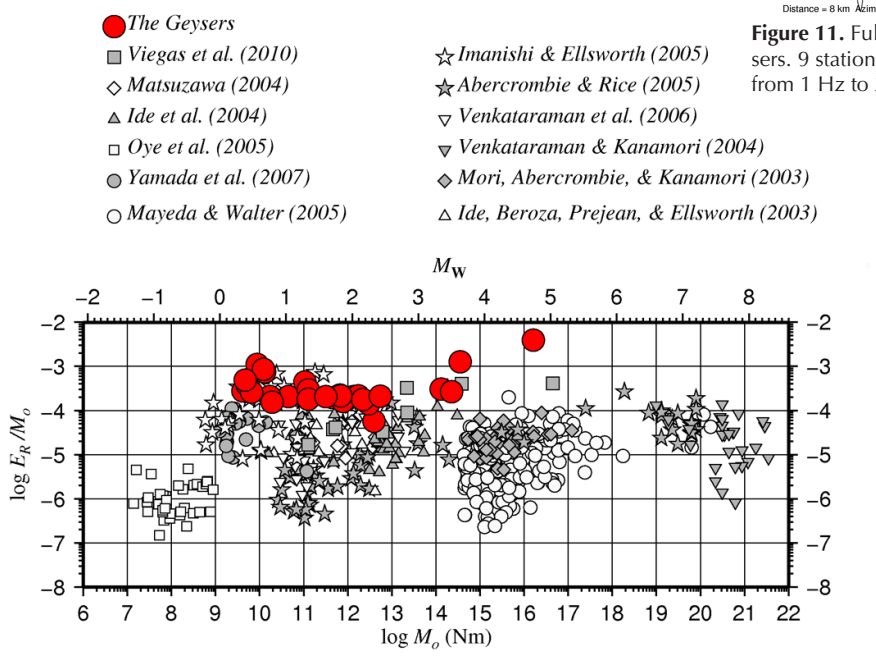

Figure 10. Radiated energy over seismic moment obtained for all the micro-earthquakes in the dataset, using the NetMoment method ploted together with a compilation of other studies.

Moment Tensor Inversion

We started performing the full second-order Moment Tensor (MT) inversion, following the method of Minson and Dreger (2008). The method allows solving for the standard deviatoric component and for the isotropic component. Substantial volumetric components have been found for earthquakes in geothermal and volcanic environments (*e.g.*, Julian *et al.*, 1998), including The Geysers (Boyd 2011, Ross *et al.*, 1996), possible linked with the presence of fluids.

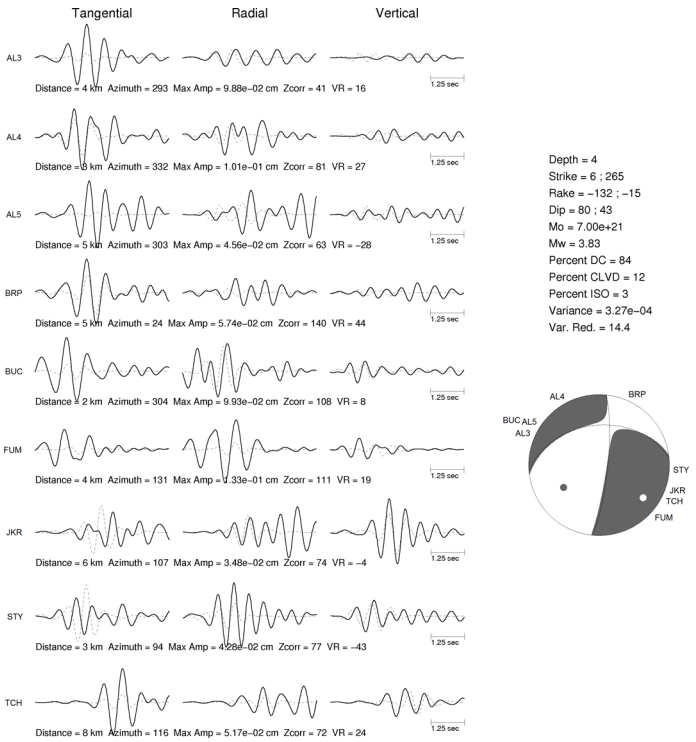

Figure 11. Full Moment Tensor solution for a M3 earhquake at The Geysers. 9 stations are used in the inversion. The waveforms are band passed from 1 Hz to 2 Hz.

Figure 11 shows a MT solution obtained for a M3 at The Geysers. This earthquake has can be fitted with a double-couple solution (84%) and shows a very small isotropic component (3%). However the quality of the fit is poor and needs to be improved. The analysis is performed at the frequency band of 1 Hz to 2 Hz, the lowest frequency for which there is enough signal o model. At these frequencies we need to generate Green's functions with a resolution of at least 1 km. We start using a one-dimensional (1D) velocity model to generate the Green's functions. We have found differences in the amplification of the signal in close by stations, due to site effects, not capture by a 1D velocity model, and are in the process of identifying and selecting the stations with fewer reverberations. We are investigating the usefulness of using high-

frequency Green's functions obtained from a high resolution 3D local earthquake tomography.

Conclusions

We investigate the source parameters of micro-earthquakes at the Northwest Geysers near the injection well Prati 9, before and during water injection, from 2005 to 2010, looking for temporal and spatial variations.

We find a good correlation coefficient of 91% between the monthly water injection-rate and the number of induced micro-earthquakes located inside the small volume, with a zero time lag, indicating that the seismic response to water injection is less than a month time. We find the *b*-value in the Gutenberg−Richter law, which equates the proportion of small earthquakes to large ones, increased from 1.3 to 1.6 with the start of water injection, indicating an increase of the number of small earthquakes relative to larger earthquakes due to reservoir stimulation. We find that the volume of the micro-seismicity cloud correlates well with the volume of injected water, and that most large micro-earthquakes (>M2) occur near the boundaries of the micro-earthquake cloud. We notice that the shape of the earthquake cloud is slightly elongated in the SW-NE direction, consistent with the preferential alignment direction of micro-cracks found in anisotropic studies, indicating that slip is being facilitated in pre-existing cracks.

We utilize three approaches to determine the source parameters of the micro-earthquakes; the Empirical Green's Function (EGF) method (Viegas *et al.*, 2010), NetMoment method (Hutchings 2002), and moment tensor inversion (Minson and Dreger, 2008). We validate the NetMoment method by applying the EGF method to a common set of 30 micro-earthquakes. Similar measured corner frequencies and calculated attenuation quality factors validate the NetMoment approach.

Our results indicate that micro-earthquakes at the Northwest Geysers have on average stress drops (mean of 11 MPa) comparable to the ones of natural occurring tectonic micro-earthquakes in the region (around 17 MPa), similarly to the results of Hough *et al.* (1999), which used a multiple empirical Green's function approach, and found stress drops of 5.5 MPa to 110 MPa for 61 shallow (<5 km) micro-earthquakes (M0 to M1.5) occurring at the Coso Geothermal Area, CA.

We obtain high radiated energy values for the micro-earthquakes at The Geysers, but still comparable to the values obtained for natural occurring earthquakes. The high radiated energy values, associated with "normal" stress drop values, indicates that a large part of the energy budget is spent in radiated energy and not in generating new surfaces or in friction (heating), favoring the hypotheses of slip on pre-existing cracks.

We are developing the full MT inversion to better constrain the volumetric components so often found for micro-earthquakes in geothermal and volcanic environments. We are investigating possible 1D and 3D velocity models to generate Green's functions at frequencies from 1 Hz to 2 Hz. The source information has implications in the understanding of the physics of the faulting mechanism and it is useful for the assessment of the seismic potential in areas of ongoing geothermal exploration.

Acknowledgments

Moment tensors were computed using the MTPACKAGE developed by Douglas Dreger of the Berkeley Seismological Laboratory, and Green's functions were computed using the FKRPROG software developed by Chandan Saikia of URS.

References

Abercrombie, R. E., and J. R. Rice (2005). Small earthquake scaling revisited: can it constrain slip weakening? *Geophys. J. Int.*, 162, 406-424.

Boatwright, J. (1980). A spectral theory for circular seismic sources: simple estimates of source duration, dynamic stress drop, and radiated energy, *Bull. Seismol. Soc. Am.*, 70, 1-28.

Boyd, O.S., D. Dreger, M. Hellweg, J. Taggert, P. Lombard, S. Ford, and A. Nayak (2011). Deviatoric Moment Tensor Analysis at The Geysers Geothermal Field, *Seism. Res. Letters,* 82(2).

Eberhart-Phillips, D., and D. H. Oppenheimer (1986). Induced Seismicity in The Geysers Geothermal Area, California, *J. Geophys. Res.*, 91, 11463-11476.

Elkibbi, M., M. Yang and J. A. Rial (2005). Crack-induced anisotropy models in The Geysers geothermal field, *Geophys. J. Int.* 162, 1036–1048 doi: 10.1111/j.1365-46X.2005.02697.x

Eshelby, J. D. (1957). The determination of the elastic field of an ellipsoidal inclusion and related problems, *Proc. Roy. Soc. Lond., A*, 241, 376-396.

Evans, J.R., Julian, B.R., Foulger, G.R. & Ross, A., (1995). Shear-wave splitting from local earthquakes at The Geysers geothermal field, California, *Geophys. Res. Lett.,* 22(4), 501–504.

Hough, S.E., J. M. Lees, and J. Monastero (1999). Attenuation and Source Properties at the Coso Geothermal Area, California, *Bull. Seism. Soc. Am*, 89(6), 1606-1619.

Hutchings, L. (2002). Program NetMoment, a Simultaneous Inversion for Moment, Source Corner Frequency, and Site Specific t*. Lawrence Livermore National Laboratory, UCRL-ID 135693.

Hutchings, L., and F. Wu (1990). Empirical Green's functions from small earthquakes – A waveform study of locally recorded aftershocks of the San Fernando earthquake, *J. Geophys. Res*., 95, 1187-1214.

Hutchings, L., K. Boyle, and S. Jarpe (2010). Near-real Time Interpretation of Microearthquake Data for Reservoir Modeling. *Geothermal Res. Council, Transactions,* 17, 2010 Annual Meeting, Sacramento, CA.

Ide, S., G. C. Beroza, S. G. Prejean and W. L. Ellsworth (2003). Apparent break in earthquake scaling due to path and site effects on deep borehole recordings, *J. Geophys. Res*., 108, doi: 10.1029/2001JB001617.

Imanishi, K., and W. L. Ellsworth (2006). Source scaling relationships of microearthquakes at Parkfield, CA, determined using the SAFOD pilot hole seismic array, in *Earthquakes: Radiated Energy and the Physics of Faulting, Geophys. Monogr. Ser.*, vol. 170, edited by R.E. Abercrombie, A. McGarr, H. Kanamori and G. Di Toro, pp. 81–90, American Geophysical Union, Washington, D.C.

Jarpe, S., L. Hutchings, K. Boyle, G. Viegas, and E. Majer (2011). Inexpensive, Easily Operated Micro-earthquake Recorders and Automated Data Processing for Rapid, High Resolution Analysis. Submitted to Journal of Geophysics (in review).

Julian, B. R., A. D. Miller, and G. R. Foulger (1998). Non-double-couple earthquakes I. Theory, *Rev. Geophys*., 36, 525-549.

Karner, S. L. (2005). Stimulation techniques used in enhanced geothermal systems: perspectives from geomechanics and rock physics, *Proceedings, 30th Workshop on Geothermal Reservoir Engineering*, Stanford University, Stanford, CA, SGP-TR-176.

Madariaga, R. (1976). Dynamics of an expanding circular crack, *Bull. Seism. Soc. Am*., 66, 639-666.

Majer, E.L, R. Baria , M. Stark, S. Oates, J. Bommer, B. Smith and H. Asanuma (2007b). Induced seismicity associated with Enhanced Geothermal Systems, *Geothermics*, 36, 185-227.

Majer, L. E., and J. E. Peterson (2007a). The impact of injection on seismicity at The Geysers, California Geothermal Field, *Int. J. Rock Mech. Mining Sci.*, 44, 1079-1090.

Minson, S. and D. Dreger (2008). Stable inversions for complete moment tensors *Geophys J. Int.,* doi: 10.1111/j.1365-246X.2008.03797.x

Mori, J. J., and A. Frankel (1990). Source parameters for small events associated with the 1986 North Palm Springs, California, earthquake determined using empirical Green functions, *Bull. Seism. Soc. Am*., 80, 278-295.

Ross, A., G. R. Foulger, and B. R. Julian (1999). Source processes of industrially induced earthquakes at The Geysers geothermal area, California, *Geophysics*, 64, 1877-1889.

Smith, J. L. B., J. J. Beall, and M. A. Stark (2000). Induced seismicity in the SE Geysers field, *Geothermal Resources Council Transactions*, 24, 24-27.

Viegas, G. (2011). Source parameters of the July 16 2010 M3.4 Germantown, MD, Earthquake, Submited to *Seismological Research Letters*.

Viegas, G., Hutchings, L. J. (2010). Source Characteristics of Microearthquakes at the Northwest Geysers Geothermal Field, California, *Geothermal Resources Council Transactions*, 34, 1265-1272.

Viegas, G., R. E. Abercrombie and W.-Y. Kim (2010). The 2002 M5 Au Sable Forks, NY, earthquake sequence: source scaling relationships and energy budget, *J. Geophys. Res.* (in press).

Yamada, T., J. J. Mori, S. Ide, R. E. Abercrombie, H. Kawakata, M. Nakatani, Y. Iio, and H. Ogasawara (2007). Stress drops and radiated seismic energies of microearthquakes in a South African gold mine, *J. Geophys. Res.*, 112, B03305, doi: 10.1029/2006JB004553.